Electrical transport and thermometry of electroformed titanium dioxide memristive switches

Julien Borghetti,[a] Dmitri B. Strukov, Matthew D. Pickett, J. Joshua Yang, Duncan R. Stewart, and R. Stanley Williams[b]
Information and Quantum Systems Lab, Hewlett-Packard Laboratories, 1501 Page Mill Road, Palo Alto, California 94304, USA

(Received 25 June 2009; accepted 20 October 2009; published online 22 December 2009)

We investigated the electrical transport of electroformed titanium dioxide memristive switches from liquid helium to room temperatures in order to better understand their internal states. After electroforming, we observed a continuous transition between two distinct limiting behaviors: a nearly Ohmic "ON"-state and an "OFF"-state characterized by conduction through a barrier. We interpret our data in terms of a model in which the electroforming step creates a conducting channel that does not completely bridge the metal contacts on the titanium dioxide film. The switching then occurs as a result of voltage-induced changes in the oxygen vacancy concentration in the gap between the tip of the channel and the adjacent metal contact. We used the metallic resistivity of the conduction channel as an *in situ* thermometer to measure the local device temperature, thus revealing an important implicit state variable. © *2009 American Institute of Physics*. [doi:10.1063/1.3264621]

I. INTRODUCTION

Voltage-polarity dependent resistive switching has been observed and reported by numerous researchers since Hickmott in 1964.[1–3] Recently, we identified such bipolar switches as a type of memristor,[4] or more properly a memristive device,[5] and provided a minimal physical model for their dynamical behavior.[6,7] This identification provides the mathematical foundation for incorporating these bipolar switches into electronic circuit designs.[4,5,8] The defining equations for a memristive device are the following.[5]

$$v = R(\mathbf{w},i)^{*}i, \tag{1}$$

$$d\mathbf{w}/dt = f(\mathbf{w},i), \tag{2}$$

where v is the voltage and Eq. (1) defines the generalized resistance R of the device as a function of the current i [thus, the current-voltage (i-v) relation is explicitly nonlinear, and it must obey the restriction that $v=0$ when $i=0$ and vice versa; pure memristive devices do not store energy] and one or more continuous *state variables* represented by $\mathbf{w}$, which are defined by the dynamical relation Eq. (2).

The property of state is critical to understand the nature and uniqueness of bipolar switches as two-terminal dynamical devices. We thus investigated the quasistatic transport properties [e.g. Eq. (1)] of a set of titanium dioxide bipolar switches in order to provide a physical picture of the various states of these memristive devices. This test-bed material can exhibit either bipolar or unipolar switching[2,9] over a wide range of current and thus electrical power. Unipolar switching requires only a single voltage polarity to toggle a device into its ON or OFF resistance state.[10,11] Joule heating has been implicated in the mechanism of unipolar switching,[3] and this has been confirmed experimentally.[12,13] In contrast, bipolar switching requires opposite polarity voltages to switch between ON and OFF resistance states. In such devices, it has not been clear if resistance switching is assisted by Joule heating, in particular because bipolar switching typically requires smaller currents.[14,15]

The local temperature increase during switching may be influential in determining the dynamical characteristics of a device. For example, one of the most challenging figures of merit for a memory or storage device is the relationship between switching speed and state retention time at the operating temperature.[16,17] For a storage application, one may desire gigahertz switching operation and >10 years retention time.[3,10,11,16] For a device in which the switching mechanism depends upon the drift of charged dopant species,[17] this large dynamic range has been shown theoretically to be possible for systems in which the usual linear relation between dopant drift velocity and internal electric field breaks down at high fields and/or there is internal heating caused by electrical current flow. Thus, identification of self-heating and a means to determine the temperature, which then becomes a state variable for the system, is important.

Our primary characterization technique in the study reported here was temperature-dependent transport measurements of thin film memristive switches that had been prepared in a variety of states, from the virgin or pre-electroformed condition all the way to a dead short.[18] We observed the signature of specific electron transport regimes, including a transition from metallic to electron barrier tunneling at zero bias, which allowed us to infer the electronic microstructure of the device. Additionally, we used the metallic resistance as an *in situ* thermometer, which enabled us to measure the internal device temperature as a function of current for various quasistatic states and determine a simple physical model for the relationship.

[a]Electronic mail: julien.borghetti@hp.com.
[b]Electronic mail: stan.williams@hp.com.

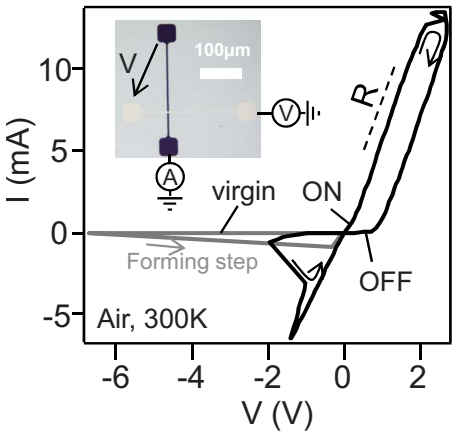

FIG. 1. (Color online) Current vs externally applied voltage plots for conventional electroforming and switching behavior of a TiO_2 memristive switch. (Inset) Optical micrograph of a junction showing the connecting wires and contact pads, with the four-wire measurement scheme illustrated schematically. The dark color of the bottom electrode is caused by the blanket film of TiO_2 that was deposited over the entire substrate.

II. EXPERIMENTAL DETAILS

A typical device examined in this work is shown in the inset of Fig. 1. On an oxidized silicon wafer, a Ti adhesion layer (5 nm) and the bottom Pt electrode (15 nm) were electron-beam evaporated through a shadow mask. Then, the titanium dioxide layer (35 nm) was sputtered in 3 mtorr Ar from a rutile polycrystalline target over the entire substrate, held at 250 °C. Previous studies showed that the as-deposited film was amorphous with an oxygen to titanium ratio close to 2.0.[7] Finally, the top Pt electrode (15 nm) was evaporated directly onto the titanium dioxide through the shadow mask oriented at a right angle to the bottom electrode. The top and bottom electrode widths were ~10 μm in order to yield a measurable electronic current at low temperatures for some of the device states that were studied. We recognize that the quantitative details will change for smaller device dimensions, but we wanted to obtain a consistent picture of the wide range of properties that are observable from a single device structure. The electrical measurements were performed using an Agilent 4156 semiconductor parameter analyzer and the four-wire method to eliminate the resistance of the leads, with the bottom electrode grounded (illustrated in the inset in Fig. 1). In this paper, the applied voltage is called the external voltage, and the voltage drop across the vertical junction determined from four-wire measurements is called the internal voltage, which is used in the plots of results in Figs. 2 and 3. The samples were wire bonded and mounted in the helium flow of a cryostat (Oxford VTI51/30). The data presented in Figs. 1–3 were collected from three different devices, but the behavior of all the samples was consistent.

The current-voltage (i-v) characteristics for device electroforming and switching in ambient conditions are shown in Fig. 1. A device was electroformed by sweeping the external voltage to ~−7 V, shown as the gray trace in Fig. 1, which irreversibly transformed the device from its as-fabricated low-bias resistance (~10^8 Ω) to a significantly less resistive regime. After the electroforming procedure, each device was

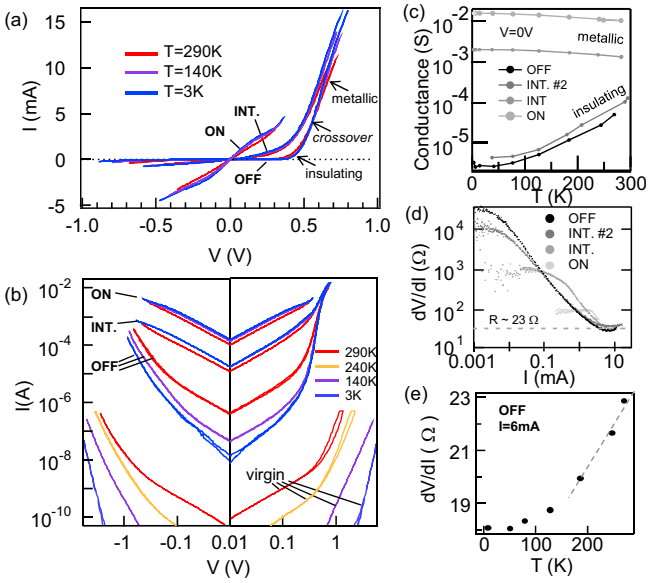

FIG. 2. (Color online) (a) Four wire current-voltage measurement at various temperatures and various states: ON, intermediate (INT.), and OFF. The crossover indicated by the black dotted horizontal line denotes a boundary between insulating and metallic currents. (b) Same data as (a) plotted on a log-log scale and compared with measurements from the virgin state. (c) At zero bias (0–50 mV), the temperature dependence of the conductance is metallic for the ON states and insulating in the OFF states. (d) The differential resistance (dv/di) is state dependant at low current and invariant (R ~23 Ω) at large current. (e) The temperature dependence of the high-current resistance R is metallic (the dashed line shows a temperature coefficient $\alpha = 1.5 \times 10^{-3}$/K).

cycled reversibly and continuously between a higher resistance (~10^5 Ω), which we defined as the OFF state, and a lower resistance (~100 Ω), defined as the ON state, several times by the application of positive and negative voltages, respectively.[7] Since the resistance switching is continuous, the choice of OFF and ON states is actually a matter of convenience. We chose two states with very different transport properties that could be reproducibly accessed by the simple application of an appropriate voltage (+9 V external, +2 V internal for OFF and −4 V external, −2 V internal for ON). Current-voltage measurements to characterize the quasistatic states of the devices were performed at internal voltage magnitudes less than 1 V, which were too small to induce perceptible changes, with the OFF-like states probed at positive bias and the ON-like states at negative bias to minimize inadvertent switching. The application of a large negative voltage would drive the device resistance to a value of ~10 Ω, which we termed a shorted state since such a device could not be reset to a higher resistance value.

III. RESULTS

A. Electrical transport

A consistent set of representative i-v characteristics of a particular device configured in several different states collected at selected temperatures from 290 to 3 K are shown in Figs. 2(a) and 2(b). In the virgin state, the conduction was thermally activated, with the apparent activation energy varying from roughly 500 to 200 meV when cooling from room to liquid nitrogen temperatures. This behavior is typi-

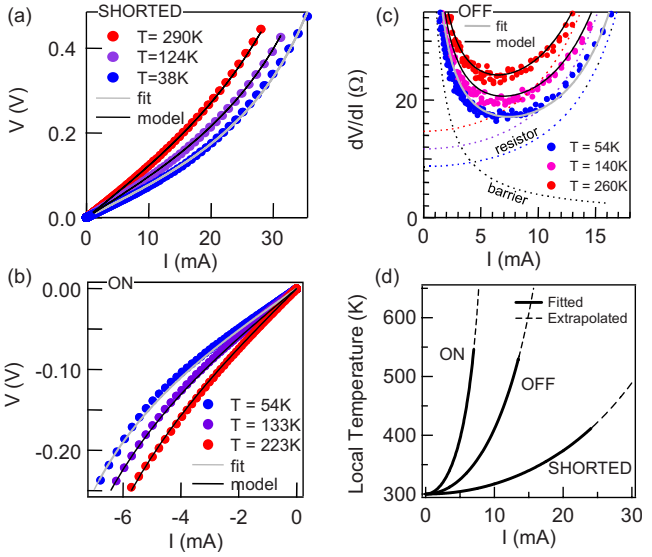

FIG. 3. (Color online) (a) A shorted junction—a large negative bias switched the junction to a $R_{0\ V}=12\ \Omega$ irreversible state—has a metallic behavior that deviates from ohms law. The solid lines show a fit to and calculations from the self-heating mode described in the text. (b) A reversible ON state ($R_{0\ V}=40\ \Omega$) also shows a deviation from ohms law that also be explained by self-heating. (c) For the OFF state, the differential resistance dv/di is plotted vs current in order to discriminate the temperature independent tunneling from the metallic temperature-dependent and self-heating regime at higher current. (d) Estimated effective or average local temperatures inside the devices for different states as a function of the current.

cal for bulk transport in amorphous or nanocrystalline insulators, where the disorder dominates over the band structure.[19,20] In particular, the power-law behavior ($i\sim v^{\alpha}$ with $\alpha\sim 5$) at large bias is frequently reported for varistors.[21] Even though this power law is consistent with bulk-limited conduction and the device fabrication would appear to produce symmetric metal contacts, the *i-v* characteristics were significantly rectifying.[22] This behavior has previously been shown to result from the fact that some Ti from the adhesion layer diffuses through the bottom Pt electrode to form a lower-barrier contact by inducing oxygen vacancies in the titanium dioxide, while the top contact is Schottky-like.[7]

After the device has been electroformed, the temperature dependence of the conduction is dramatically weaker, as seen in Fig. 2(a). The electronic transport is fundamentally different, which is expected since electroforming is a traumatic experience that results in the formation of (usually) a single dominant nanoscale conducting channel, even on a large area device.[23–28] Here, we use our transport results to refine this general picture.

The temperature dependence of the low-bias resistance of several states is displayed in Fig. 2(c). Close to the OFF state, the net device resistance increased moderately as temperature decreased. This weak thermal activation and the nonlinear *i-v* characteristics are signatures of some form of electron tunneling through a thin insulator.[29,30] Close to the ON state, the temperature dependence of the resistance was initially metallic, decreasing with decreasing temperature with a relative temperature coefficient $\alpha=1.5\times10^{-3}/\mathrm{K}$ ($\pm0.1\times10^{-3}$), and then saturating at about 40 K. This α value falls in the range of a typical metal or degenerate semiconductor.

The electronic transport at large bias reveals some surprising behavior [Figs. 2(a) and 2(b)]. The *i-v* curve of the OFF-state becomes linear at large bias with a slope comparable to the intermediate state. Additionally, close to the OFF state, the current is weakly thermally activated (insulating) at low bias but thermally inhibited (metallic) above a crossover at about 3 mA. The linear behavior at large bias can also be seen in the switching curve in Fig. 1. We approximate the nonlinear transport by a simple exponential relation $i(v)=i_0(e^{v/v_0}-1)$, where i_0 and v_0 are two state-dependent parameters, and we assume that R_S is a series resistance. If we now consider the differential resistance of the two elements in series, we find $dv/di=R_S+(v_0/i_0)/(i/i_0+1)$. For large currents, dv/di is constant and equal to the series resistance, and at low currents it is dominated by the nonlinear element. The differential resistance versus current plots for four different states are displayed in Fig. 2(d), and we see that all display varying amounts of nonlinear component at low bias and then reach a minimum value in the range $R_S\sim23\ \Omega$ for this particular device. Plots of the high bias differential resistance versus temperature for all of the states reveal that this R_S has a metallic temperature coefficient α of $\sim1.5\times10^{-3}/\mathrm{K}$, essentially the same as the coefficient measured for the ON-state low-bias resistance.

B. Local heating estimation method

The pictures of the states are almost complete, but in fact there is a so-far hidden quasistatic state variable that our measurements enable us to uncover. The high-bias deviation of the *i-v* characteristics of all the states from Ohmic behavior, which is an indication of Joule heating in the metallic components of the devices, can be used as a thermometer to measure the internal temperature. Direct evidence for Joule heating was provided by a roughly ~2 degrees rise in temperature of the thermometer mounted on the crystal sample holder. This procedure is first illustrated by using a device that had been exercised by switching ON and OFF several times, and was then shorted by applying a large negative bias to create an irreversible and very low resistance state. The plots in Fig. 3(a) (v versus i in this case) are consistent with a simple thermal model. The resistance of the metallic component is described by $R(T_{\mathrm{local}})=R_{300\ \mathrm{K}}[1+\alpha(T_{\mathrm{local}}-300\ \mathrm{K})]$, where as before α is the temperature coefficient, $R_{300\ \mathrm{K}}$ is the zero bias electrical resistance at 300 K and T_{local} is the internal temperature of the component. The difference between the ambient (T_{amb}) and the internal temperatures is determined by a net thermal resistance: $T_{\mathrm{local}}=T_{\mathrm{amb}}+\mathcal{R}_{\mathrm{th}}P$, where P is the dissipated electrical power.[31,32] Hence, the *i-v* measured at T_{amb} is described by

$$v=\frac{R_{300\ \mathrm{K}}[1+\alpha(T_{\mathrm{amb}}-300\ \mathrm{K})]}{1-\alpha R_{300\ \mathrm{K}}\mathcal{R}_{\mathrm{th}}i^2}i. \tag{3}$$

For the shorted device, the 300 K electrical resistance is $R_{300\ \mathrm{K,shorted}}=12\ \Omega$. Using this measured value and the known value of α, a single parameter fit of the $T=38$ K *i-v*

curve yielded a thermal resistance $\mathcal{R}_{\text{th,shorted}}=21$ K/mW. Using the three parameters thus determined, we then calculated the *i-v* curves at 124 and 290 K, and the agreement with the experimental data shown in Fig. 3(a) is convincing support for this model.

We then applied this approach to the ON state, where comparable effects were observed for currents between −6 and 6 mA. We measured the net electrical resistance $R_{300\ \text{K,ON}}=40\ \Omega$ at 300 K. Using the known α value, we performed a fit to the *i-v* data at $T=54$ K and found that the thermal resistance of the bridging channel was $\mathcal{R}_{\text{th,ON}}=210$ K/mW. We then calculated the *i-v* curves at 133 and 233 K, and the results shown in Fig. 3(b) support this ON-state model.

The Joule-heating model was finally applied to the junction in the OFF state. However, the *i-v* shapes are dominated by the barrier transport at low bias, so we examined the differential resistance. Since the *i-v* characteristics are temperature independent in the nonlinear resistance regime ($50\ \mu\text{A} < i < 1$ mA), we described the barrier transport with the temperature invariant exponential and included self-heating effects in only the metallic component, obtaining the following expression:

$$dv/di = (v_0/i_0)/(i/i_0+1) + \frac{R_{300\ \text{K}}[1+\alpha(T_{\text{amb}}-300\ \text{K})]}{(1-\alpha R_{300\ \text{K}}\mathcal{R}_{\text{th}}i^2)} + \frac{2\alpha R_{300\ \text{K}}{}^2\mathcal{R}_{\text{th}}[1+\alpha(T_{\text{amb}}-300\ \text{K})]i^2}{(1-\alpha R_{300\ \text{K}}\mathcal{R}_{\text{th}}i^2)^2}. \quad (4)$$

The barrier transport parameters i_0 and v_0 were fitted at 54 K and low current [see extrapolated black dashed line in Fig. 3(c)]. The value of α was the same as above, and the electrical resistance and thermal resistance of the OFF state metallic component were found to be $R_{300\ \text{K}}=16\ \Omega$ and $\mathcal{R}_{\text{th,OFF}}=60$ K/mW by fitting the data to Eq. (4). The parameters thus determined were used to calculate the *i-v* curves at $T=140$ and 260 K, and are compared with the experimental data in Fig. 3(c).

We can now compute the effective internal temperature as a function of the measured current [Fig. 3(d)] for the states that have been analyzed. The internal heating is the square of the current times the product of the electrical and thermal resistances: $T_{\text{local}}=T_{\text{amb}}+[(\mathcal{R}_{\text{th}}R_{300\ \text{K}}[1+\alpha(T_{\text{amb}}-300\ \text{K})]i^2)/(1-\alpha R_{300\ \text{K}}\mathcal{R}_{\text{th}}i_2)]$. In the shorted state, the heating is lowest because of the combination of a low electrical resistance and thermal resistance.

IV. DISCUSSION AND SUMMARY

Schematic illustrations of the virgin, OFF and ON states of the electroformed devices are shown in Fig. 4. With respect specifically to the measured electrical characteristics of the device shown in Fig. 3, the electroforming step created a conducting channel with an electrical resistance of $R_S=16\ \Omega$, as determined from measurements of the series Ohmic resistance of the OFF state. A previous study of similar devices for which the top electrode was delaminated has indicated that a typical channel has a diameter of ~100 nm.[23] There is a gap of width *w*, which we estimate to

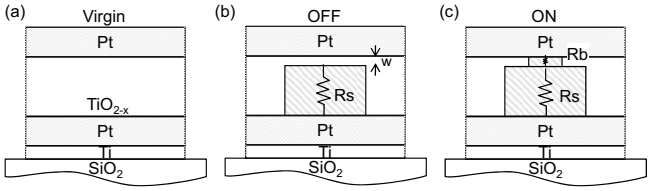

FIG. 4. (a) Schematic of the active region cross section in the virgin state. (b) In the OFF state, a resistance R_S of the electroformed metallic channel is in series with a tunneling gap having a width *w*. (c) A metallic channel R_b bridges the gap in the ON state.

be $\sim 2 \pm 1$ nm, between the top of the channel and the bottom of the metal contact that acted as a tunnel barrier in the OFF state. Thus, the conducting channel was approximately disk-shaped with a height of ~33 nm, implying an electrical resistivity of $\sim 4\times 10^{-4}\ \Omega$ cm, which is consistent with a conductive titanium oxide. The measured net resistance of the ON state of this device was 40 Ω, which indicated that there was a nearly Ohmic bridge across the gap with an electrical resistance of $R_b \approx 24\ \Omega$ in series with the conducting channel. The thermal resistance of the OFF state, 60 K/mW, was dominated by heat conduction through the bottom of the conducting channel to the lower metal contact, whereas the thermal resistance of the ON state, 210 K/mW, was mainly due to the conducting bridge. The observation that the internal effective temperature was higher for the ON state device compared to the OFF state device for the same current was caused by the Joule heating in the Ohmic bridge R_b for the former, whereas in the latter the electrons tunneled through the insulating gap and deposited their energy directly into the metal contact.

We thus see that the state of a titanium dioxide electroformed memristive switch can be tuned from metallic conduction to barrier transport, both in series with a metallic conducting channel. We identified temperature as an important hidden state variable in this system, and measured an effective or average internal temperature as a function of device current based on the steady-state deviation of the high bias resistance from Ohmic behavior. These insights may prove useful in the design of bipolar switching devices that require a very large ratio of state retention to switching times.

ACKNOWLEDGMENTS

We acknowledge technical assistance from Cuong Le. We also acknowledge numerous helpful discussions with John-Paul Strachan, Gilberto Medeiros-Ribeiro, Philip J. Kuekes, and Alexander M. Bratkovsky.

[1] W. R. Hiatt and T. W. Hickmott, Appl. Phys. Lett. **6**, 106 (1965).
[2] F. Argall, Solid-State Electron. **11**, 535 (1967).
[3] G. Dearnaley, A. Stoneham, and D. Morgan, Rep. Prog. Phys. **33**, 1129 (1970).
[4] L. O. Chua, IEEE Trans. Circuit Theory **18**, 507 (1971).
[5] L. O. Chua and S. M. Kang, Proc. IEEE **64**, 209 (1976).
[6] D. B. Strukov, G. S. Snider, D. R. Stewart, and R. Stanley Williams, Nature (London) **453**, 80 (2008).
[7] J. J. Yang, M. D. Pickett, X. Li, D. A. A. Ohlberg, D. R. Stewart, and R. S. Williams, Nat. Nanotechnol. **3**, 429 (2008).
[8] J. Borghetti, Z. Li, J. Straznicky, D. A. A. Ohlberg, D. R. Stewart, and R. S. Williams, Proc. Natl. Acad. Sci. U.S.A. **106**, 1699 (2009).

[9]D. Jeong, H. Schroeder, and R. Waser, Electrochem. Solid-State Lett. **10**, G51 (2007).
[10]R. Waser and M. Aono, Nature Mater. **6**, 833 (2007).
[11]A. Sawa, Mater. Today **11**, 28 (2008).
[12]U. Russo, D. Lelmini, C. Cagil, A. L. Lacaita, S. Spiga, C. Wiemer, M. Perego, and M. Fanciulli, Tech. Dig. - Int. Electron Devices Meet. **2007**, 775.
[13]S. Chang, S. C. Chae, S. B. Lee, C. Liu, T. W. Noh, J. S. Lee, B. Kahng, J. H. Jang, M. Y. Kim, D. -W. Kim, and C. U. Jung, Appl. Phys. Lett. **92**, 183507 (2008).
[14]C. Schindler, M. Weides, M. N. Kozicki, and R. Waser, Appl. Phys. Lett. **92**, 122910 (2008).
[15]M. Janousch, G. I. Meijer, U. Staub, B. Delley, S. F. Karg, and B. P. Andreasson, Adv. Mater. **19**, 2232 (2007).
[16]N. Das, S. Tsui, Y. Y. Xue, Y. Q. Wang, and C. W. Chu, Phys. Rev. B **78**, 235418 (2008).
[17]D. B. Strukov and R. Stanley Williams, Appl. Phys. A: Mater. Sci. Process. **94**, 515 (2009).
[18]A. Ansari and A. Qadeer, J. Phys. D **18**, 911 (1985).
[19]A. Jonscher, J. Electrochem. Soc. **116**, 217C (1969).
[20]R. Hill, Thin Solid Films **12**, 367 (1972).
[21]M. Yan and W. Rhodes, Appl. Phys. Lett. **40**, 536 (1982).
[22]T. Choi, S. Lee, Y. J. Choi, V. Kiryukhin, and S. -W. Cheong, Science **324**, 63 (2009).
[23]J. J. Yang, F. Miao, M. D. Pickett, D. A. A. Ohlberg, D. R. Stewart, C. N. Lau, and R. Stanley Williams, Nanotechnology **20**, 215201 (2009).
[24]C. Lau, D. R. Stewart, R. Stanley Williams, and M. Bockrath, Nano Lett. **4**, 569 (2004).
[25]K. Szot, W. Speier, R. Carius, U. Zastrow, and W. Beyer, Phys. Rev. Lett. **88**, 075508 (2002).
[26]K. Szot, W. Speier, G. Bihlmayer, and R. Waser, Nature Mater. **5**, 312 (2006).
[27]F. Miao, D. Ohlberg, D. R. Stewart, R. Stanley Williams, and C. N. Lau, Phys. Rev. Lett. **101**, 016802 (2008).
[28]K. Terabe, T. Hasegawa, T. Nakayama, and M. Aono, Nature (London) **433**, 47 (2005).
[29]Y. Xu, D. Ephron, and M. Beasley, Phys. Rev. B **52**, 2843 (1995).
[30]R. Martel, T. Schmidt, R. L. Sandstrom, and Ph. Avouris, J. Vac. Sci. Technol. A **17**, 1451 (1999).
[31]P. Kim, L. Shi, A. Majumdar, and P. L. McEuen, Phys. Rev. Lett. **87**, 215502 (2001).
[32]J. Gibbons and W. Beadle, Solid-State Electron. **7**, 785 (1964).